
Imaging of Extrarenal Spread, Fistulising and Atypical Pyelonephritis

10

Massimo Tonolini

10.1 Emphysematous Pyelonephritis

As mentioned in the introductory chapter of this book, diabetes mellitus (DM) is a common predisposing factor in patients with complicated urinary tract infections (UTI). Compared to the general population, diabetics and particularly those with uncontrolled DM frequently experience more severe pyelonephritis with a similar mortality rate but poorer treatment outcome, common worsening of renal function and greater need for nephrectomy [1, 2].

A rare yet characteristic form of complicated UTI, emphysematous pyelonephritis (EPN) affects diabetics in the vast majority (90%) of cases with a 3:1 female predominance; the rare nondiabetic occurrences are related to either immunosuppression or urinary tract obstruction. EPN is a severe necrotizing renal infection with a complex pathogenesis involving a combination of factors, namely, gas-forming bacteria, high tissue glucose level, impaired tissue perfusion and defective immune response. The commonest pathogens isolated from pus cultures include

Escherichia coli (49–71% of cases), *Klebsiella pneumoniae* (19%) and *Proteus mirabilis* (17%) in descending order of frequency, with frequent antibiotic resistance [3–6].

The clinical presentation is similar to that of severe forms of bacterial acute pyelonephritis (APN) and mostly includes fever, chills, flank pain, dysuria and pyuria. The usual laboratory abnormalities include leukocytosis, thrombocytopenia and altered renal function. Timely diagnosis is crucial, since untreated EPN generally progresses to sepsis and is potentially lethal [3–8].

The diagnostic hallmark of EPN is represented by abnormal gas collections within the renal parenchyma and sometimes also perinephric space. Traditionally, the usual radiographic appearance included ‘mottled’ gas over the affected kidney or crescent-shaped air collections within Gerota’s fascia corresponding to perinephric extension; however plain abdominal radiographs have moderate (70%) sensitivity for retroperitoneal air, which is commonly misinterpreted as bowel gaseous content. Ultrasound (Fig. 10.1a) may detect renal enlargement with nondependent hyperechoic foci corresponding to gas causing ‘dirty’ reverberation artefacts. Despite use of ionizing radiation, multidetector CT is by far the preferred imaging technique to diagnose EPN. Unenhanced CT images readily detect the presence, extent and position of renal gas, which may show several different patterns

M. Tonolini, M.D.
Radiology Department, “Luigi Sacco” University
Hospital, Via G.B. Grassi 74, Milan 20157, Italy
e-mail: mtonolini@sirm.org

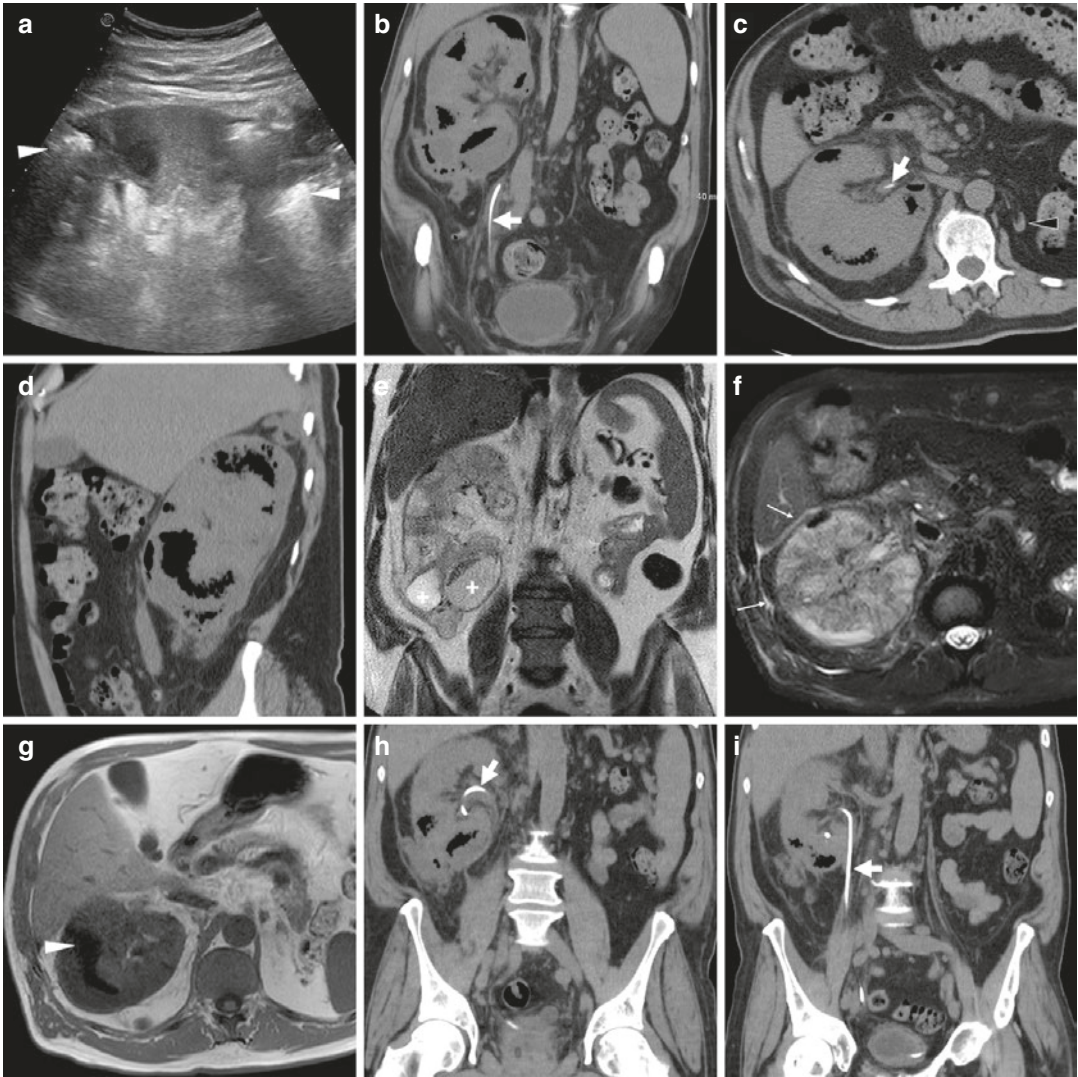


Fig. 10.1 A 63-year-old male admitted to emergency department because of high fever, dysuria and distended tender abdomen was diagnosed with decompensated diabetes mellitus, severe renal impairment (7.5 mg/dl serum creatinine), markedly increased C-reactive protein and metabolic acidosis. Initial ultrasound (**a**) showed enlargement of the right kidney, with parenchymal hyperechoic bands (arrowheads), posterior acoustic shadowing and previously unknown congenital left renal aplasia. After ureteral stenting (thick arrows), multiplanar unenhanced CT images (**a–d**) confirmed enlarged solitary right kidney with strongly hypoattenuating gaseous components, con-

sistent with emphysematous pyelonephritis. MRI follow-up (**e–g**) better showed parenchymal oedema of the right kidney, intraparenchymal fluid collections (plus in T2-weighted image (**f**)) and ipsilateral fascial thickening (thin arrows in (**g**) with fat saturation); conversely gas was less perceptible (arrowhead in T1-weighted image (**e**)). The patient's clinical conditions and laboratory changes slowly improved during conservative treatment including haemodialysis, repeated unenhanced CT studies (**h**, **i**) showed progressive decrease of renal emphysematous changes and the patient ultimately obviated the need for nephrectomy (Adapted from Open Access Ref. no [16])

such as bubbly, linear, streaky or crescent-shaped. The use of intravenous contrast is reserved for those patients with preserved renal function. The nephrographic enhancement is dif-

fusely altered with or without focal tissue necrosis, fluid-containing abscesses and delayed excretion (Fig. 10.1). Other CT findings include variable degrees of parenchymal enlargement

and destruction and possible associated conditions such as urolithiasis and obstruction. Compared to CT, MRI (Fig. 10.1) is more sensitive for the presence of parenchymal oedema and fluid collections but is limited in the assessment of gas which has very low signal intensity [9–16].

In the past, Wan et al. differentiated type-1 EPN characterised by renal necrosis with parenchymal destruction and gas but no fluid collection, from the less aggressive type-2 EPN lacking renal or perirenal fluid collections, respectively, with 69 and 18% mortality rates. Nowadays, EPN should be more comprehensively staged according to classification proposed by Huang and Tseng (Table 10.1). Included in the staging system as grade I EPN, emphysematous pyelitis corresponds to intraluminal gas in the collecting system only and represents a milder form with better prognosis [9–16].

Alternatively, gas may be detected in the urinary tract after surgery, instrumentation or catheterisation, occasionally when fistulisation with the gastrointestinal tract occurs and exceptionally from penetrating trauma [13, 14, 16].

Nowadays, with a timely CT diagnosis, conservative management of EPN is increasingly feasible and effective, particularly in classes I and II, resulting in decreased mortality, currently below 25%. The aggressive treatment includes resuscitation, intravenous fluids and antibiotics, glycaemic control, dialysis and drainage of obstruction as needed. The risk factors for unfavourable outcome include higher CT grade, shock, emergency haemodialysis, altered senso-

rium and thrombocytopenia. However, conservative treatment fails in almost one-third of cases. Nephrectomy is not associated with improved survival and should be reserved for EPN classes III and IV with adverse prognostic factors or failed conservative treatment [3–5, 7, 16–19].

10.2 Extrarenal Spread of Acute Pyelonephritis

As discussed in the previous chapter of this book, acute pyelonephritis (APN) may worsen as tiny suppurative foci coalesce leading to the formation of variable-sized round or geographic collections: these abscesses are progressively demarcated by a more or less thick and irregular inflammatory wall. Albeit sonography may identify abscesses as hypo-anechoic cavities without internal colour flow signals, multidetector CT is by far superior in the assessment of APN complications such as abscesses (Fig. 10.2) [10–12, 20–22].

When APN is not timely recognized and treated, intrarenal abscesses may cross or rupture through the renal capsule and extend into the perirenal space and sometimes even progress to involve other retroperitoneal compartments. Perinephric abscesses (PNAs) represent organized collections of purulent material which may either result from a urinary tract infection, from superinfection of a pre-existing haematoma or urinoma or form separately from the kidney such as in haematogenous dissemination. Cross-sectional CT imaging consistently and comprehensively depicts PNAs extending from or abutting the adjacent kidney. The characteristic imaging appearance includes a central near-water hypoattenuation which occasionally contains gas bubbles, corresponding to pus and liquefaction, surrounded by a peripheral enhancing wall and by regions of decreased parenchymal enhancement reflecting non-necrotic infected kidney. Representing the hallmark of the mature abscess, the ‘rim’ enhancement may be more or less (typically several millimetres) thick, intense and often irregular (Figs. 10.2, 10.3 and 10.4). In the proper clinical setting, the CT diagnosis of PNA is relatively straightforward and dictates appropriate

Table 10.1 Classification of emphysematous pyelonephritis proposed by Huang and Tseng (Adapted from Open Access Ref. no [16])

Class	Description
I	Emphysematous pyelitis—gas in collecting system only
II	Intraparenchymal gas only (no extrarenal involvement)
IIIA	Gas extending into the perinephric space
IIIB	Extension of gas into the pararenal spaces
IV	Emphysematous pyelonephritis in solitary kidney or bilateral involvement

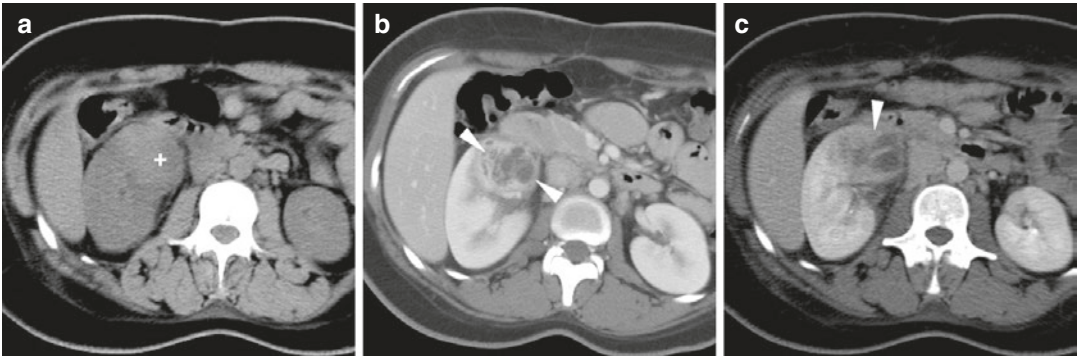


Fig. 10.2 An 18-year-old female with clinical and laboratory signs of acute urinary infection and inconclusive ultrasound findings underwent unenhanced (a) and post-contrast (b) multidetector CT. The anterior labrum of the right kidney showed mixed attenuation enlargement (plus) with nonenhancing centre and thin, irregular

peripheral enhancement (arrowheads) consistent with an abscess, which measured approximately 4×3 cm and protruded ventromedially into the perinephric space. Repeated contrast-enhanced CT (c) showed decreased size and purulent content of the abscess after antibiotic therapy

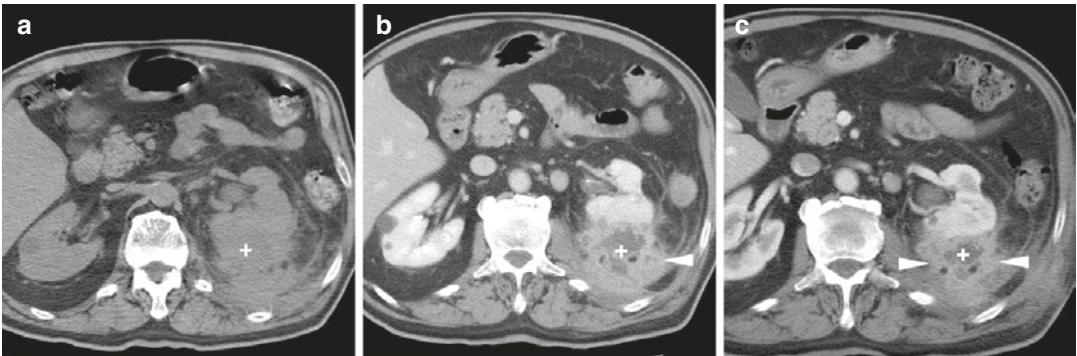


Fig. 10.3 In a 72-year-old male with history of urolithiasis and recurrent urinary infections, unenhanced (a) and post-contrast (b) CT acquisitions showed extensive inhomogeneous abnormality of the posterior aspect of the left kidney (plus) which largely occupied the dorsal perinephric and posterior pararenal spaces, thus displacing ven-

trally the kidney. The very thick, irregular peripheral enhancement (arrowheads) and fluidlike content were consistent with an abscess. Despite mild size decrease at follow-up CT (c) after 3 weeks of in-hospital treatment, nephrectomy was ultimately performed to relieve the infection

treatment with image-guided percutaneous drainage plus antibiotics [10–12, 20–22].

As discussed in the appropriate chapter of this book, although hampered by longer examination time and need for cooperation, MRI is an increasingly attractive option to comprehensively image renal infections without the use of ionizing radiation. At MRI, the mature renal abscess appears as a fluid collection with fluidlike high T2-weighted signal and internal restricted diffusion, surrounded

by a variably thick capsule with relatively lower signal intensity which enhances strongly after gadolinium contrast (Fig. 10.5) [21, 23].

The most important differential diagnoses of a PNA include:

- (a) Haematomas
- (b) Urinomas (Fig. 10.6)
- (c) Complex cystic masses (Fig. 10.7a–c)
- (d) Necrotic renal tumours (Fig. 10.7d–f)

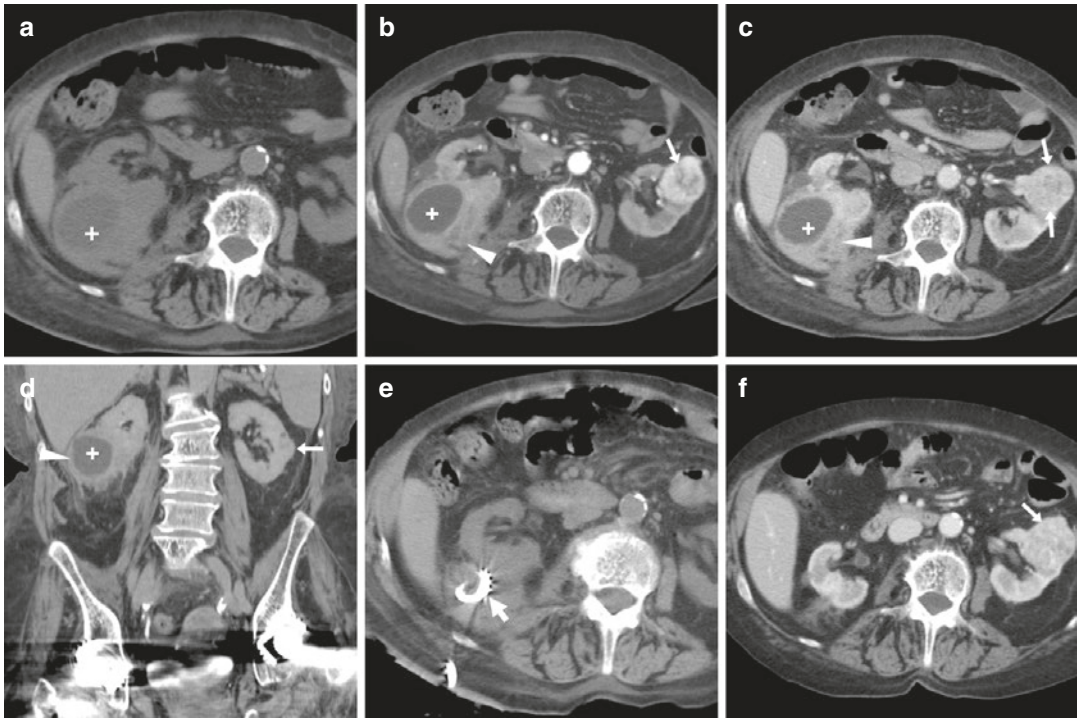


Fig. 10.4 In a 73-year-old diabetic woman hospitalized because of malaise and weight loss, unenhanced (a) and post-contrast (b–d) multidetector CT showed anterior displacement of the right kidney by a 7-cm hypoattenuating mass (plus) with nonenhancing fluid content (plus) and uneven peripheral enhancement (arrowheads), consistent

with perinephric abscess. The abscess was treated by percutaneous drainage (thick arrow in (e)) and ultimately resolved (f). The incidentally detected 3-cm left renal mass with strong, early enhancement (arrows) consistent with renal cell carcinoma was subsequently treated by nephrectomy

Apart from the trauma setting, a perinephric haematoma may result from ruptured neoplasms (particularly angiomyolipoma), vascular lesions (such as aneurysms, arteriovenous malformations or vasculitides), bleeding diathesis or excessive anticoagulation: the diagnosis is suggested by acute clinical manifestations, dropping haematocrit and by the fact that thickened perirenal septa and acute haematoma have higher unenhanced attenuation than the renal parenchyma [24–27].

Urinomas may develop after iatrogenic injury or trauma or result from increased intraluminal pressure secondary to acute or chronic obstructive uropathy. The extravasated urine shows near-water CT attenuation and MRI signal intensity, but chronic urinomas may appear as complex fluid

collections with enhancing rim and septa from chronic inflammation; the diagnostic hallmark of a urinoma is its opacification on delayed excretory-phase CT acquisition (Fig. 10.6) [28, 29].

Finally, rim-enhancing abscess lesions with internal inhomogeneity and thick, enhancing septa commonly raise a concern for a cystic or necrotic neoplasm which may suggest the need for biopsy or close follow-up (Fig. 10.7). The differential diagnosis of a complex cystic renal lesion requires careful assessment of presence and features of calcifications, quantification of internal attenuation and post-contrast enhancement, multiloculation, number and thickness of septa, mural thickness, nodularity and enhancement. An infectious process is suggested by the consistent clinical features and

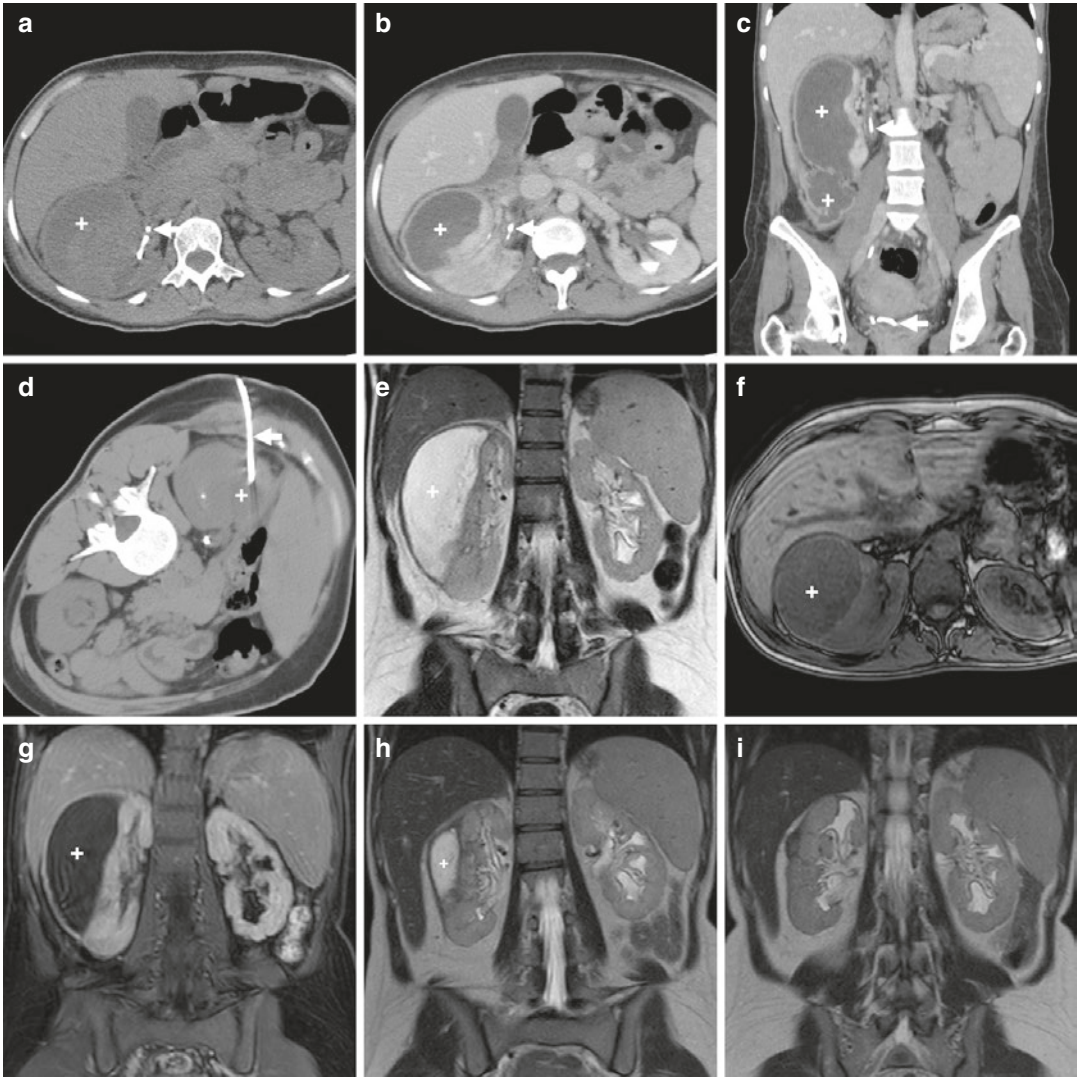


Fig. 10.5 A 37-year-old female had persistent fever and pain following right-sided lithotripsy and ureteral stenting (thick arrows) because of lithiasis and urinary infection. Unenhanced (a) and post-contrast (b, c) multidetector CT images showed severe compression of right kidney by hypoattenuating subcapsular collection (plus) with thin peripheral enhancement consistent with abscess, which extended distally to the lower renal pole into the inferior

perinephric space (c). After percutaneous CT-guided drainage (thick arrow in (d)) yielded pus, MRI showed persistence of subcapsular abscess (plus) with inhomogeneous, non-haemorrhagic content (e–g) and thin peripheral enhancement (h). MRI follow-up showed progressive decrease (plus in (h) at 8 weeks) and ultimate resolution ((i) after 4 months) of the abscess

laboratory abnormalities and by imaging detection of perinephric fat infiltration and thickening of the retroperitoneal fasciae; however, the latter findings are non-specific as they may be also seen in other conditions such as acute pancreatitis [30, 31].

10.3 Xanthogranulomatous Pyelonephritis

Xanthogranulomatous pyelonephritis (XGPN) is a rare, chronic granulomatous infection which begins in the renal pelvis and then diffuses to

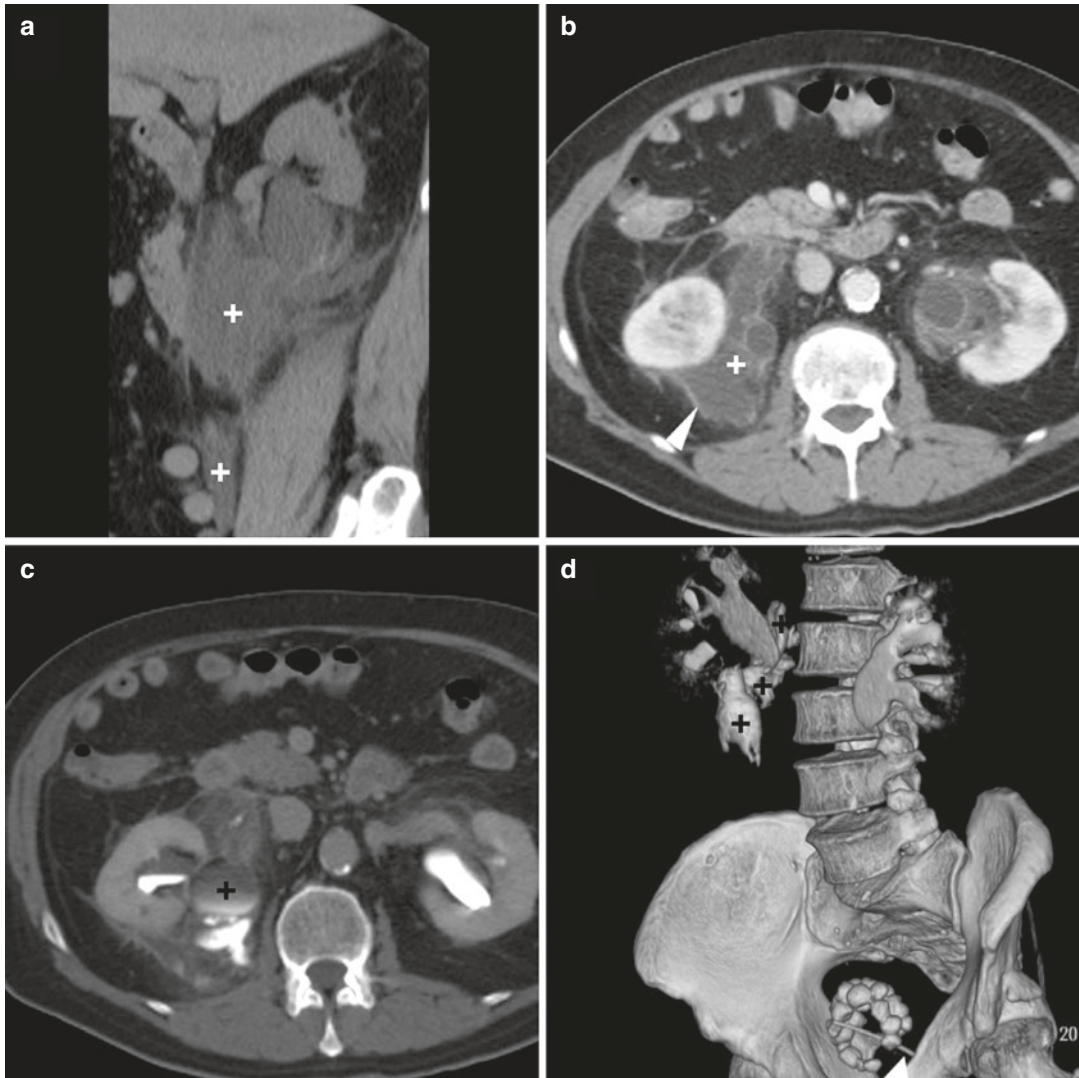


Fig. 10.6 A 70-year-old male patient with benign prostatic hyperplasia suffered from acute right flank pain. Performed to investigate suspected ureteral colic, unenhanced CT (a) showed moderate right-sided hydronephrosis plus a sizeable fluidlike collection (plus) which surrounded the renal pelvis and proximal ureter, extending into the medial perinephric space. The collection showed thin peripheral enhancement (arrowhead in (b)) after intravenous contrast which was initially interpreted as suggestive of infection. The nephrographic phase and urinary excretion were normal. Delayed phase acquisition

(c) revealed strong hyperattenuation of the perinephric and pararenal collection (plus) corresponding to extravasated urine from forniceal rupture. The urinoma (plus) was clearly depicted by three-dimensional volume rendering images (d) in its size and spatial relationship to the kidney, pelvis and proximal ureter. Note Foley catheter (thick arrow in (d)) in the bladder, filled by calculi from chronic urinary retention. The urinoma ultimately resolved on conservative treatment. (Adapted with permission from Ref. no. [53])

the medulla and cortex, leading to a progressive parenchymal destruction of the kidney which is characteristically replaced by lipid-laden 'foamy' macrophages (xanthoma cells). Further extension of XGPN to the perinephric space is commonly

encountered in approximately two-thirds of cases. The poorly understood pathogenesis involves an incomplete immune response to a subacute bacterial infection superimposed on long-standing urinary obstruction. Almost invariably unilateral,

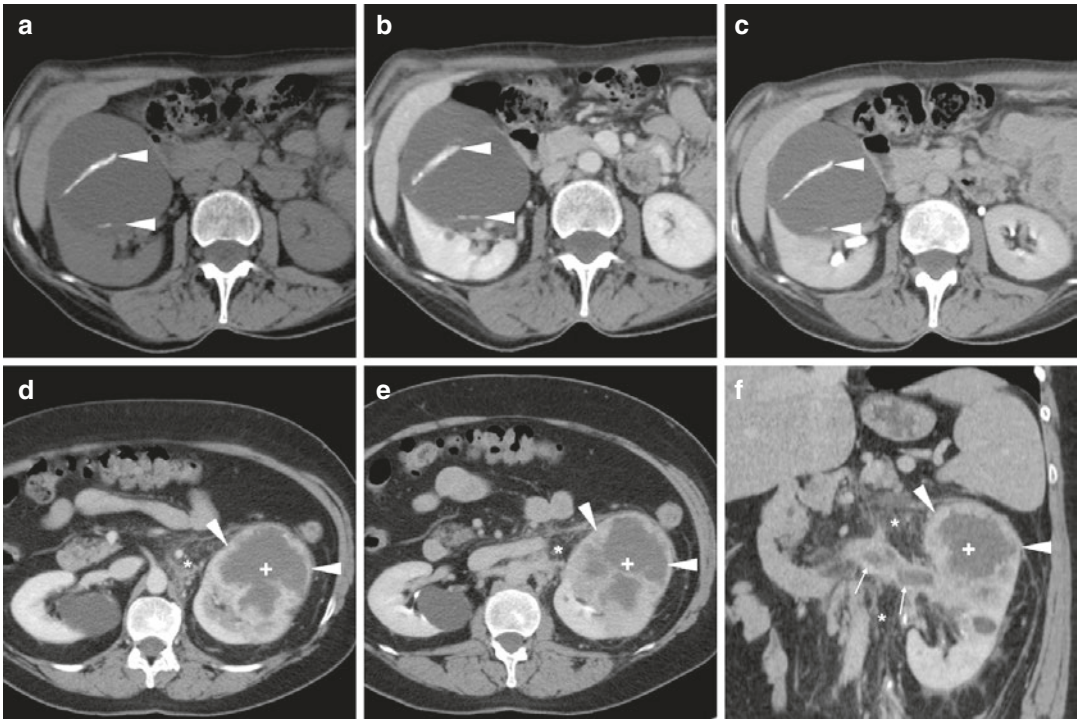


Fig. 10.7 A 62-year-old diabetic female with recurrent urinary infection was requested CT (a–c) on the basis of sonographic suspicion of renal abscess. The large right-sided renal lesion showed water-like attenuation on unenhanced scans (a), peripheral and septal calcifications (arrowheads) and absent enhancement on both nephrographic (b) and excretory phases (c), thereby excluding an infectious nature. A 58-year-old female with left-sided abdominal pain and low-grade fever underwent CT (d–f)

to investigate suspected renal colic and/or pyelonephritis. The left kidney showed a 7-cm centrally nonenhancing mass (plus) with irregular peripheral enhancement (arrowheads). Despite perinephric fat stranding (asterisk) and mild fascial thickening, the presence of ipsilateral renal vein thrombosis (thin arrows) favoured necrotic renal cell carcinoma over abscess, as confirmed at surgery and pathology

XGPN mostly occurs in middle age, with a predilection for perimenopausal women with history of urolithiasis and long-standing urinary infection or obstruction. Compared to EPN, XGPN affects diabetic patients in 10% of cases only. The clinical manifestations are non-specific, often insidious compared to the severity of the imaging abnormalities. Symptoms include low-grade fever, flank pain and tenderness, malaise, weight loss, lethargy, leukocytosis and pyuria. Sometimes a palpable mass is clinically appreciated. *E. coli* and *P. mirabilis* are the commonest identifiable microorganisms [32, 33].

In XGPN, the initial sonographic evaluation shows extensive replacement of the normal renal architecture by hypo-anechoic masses correspond-

ing to dilated calyces and abscesses filled with pus and debris (Fig. 10.11a) and amorphous central hyperechoic structures with acoustic shadowing representing ‘staghorn’ lithiasis; however these complex ultrasound findings invariably require multidetector CT for a correct characterisation, including intravenous contrast medium unless contraindicated by renal impairment. Cross-sectional imaging findings include an enlarged, non-functioning kidney with poor and heterogeneous contrast enhancement. The majority (75–90%) of cases have obstructing pelvis or ureteral lithiasis, often in a central ‘staghorn’ configuration. The destroyed parenchyma is replaced by multiple rounded hypodense cavities representing dilated, pus-filled calyces (Fig. 10.8): recognising

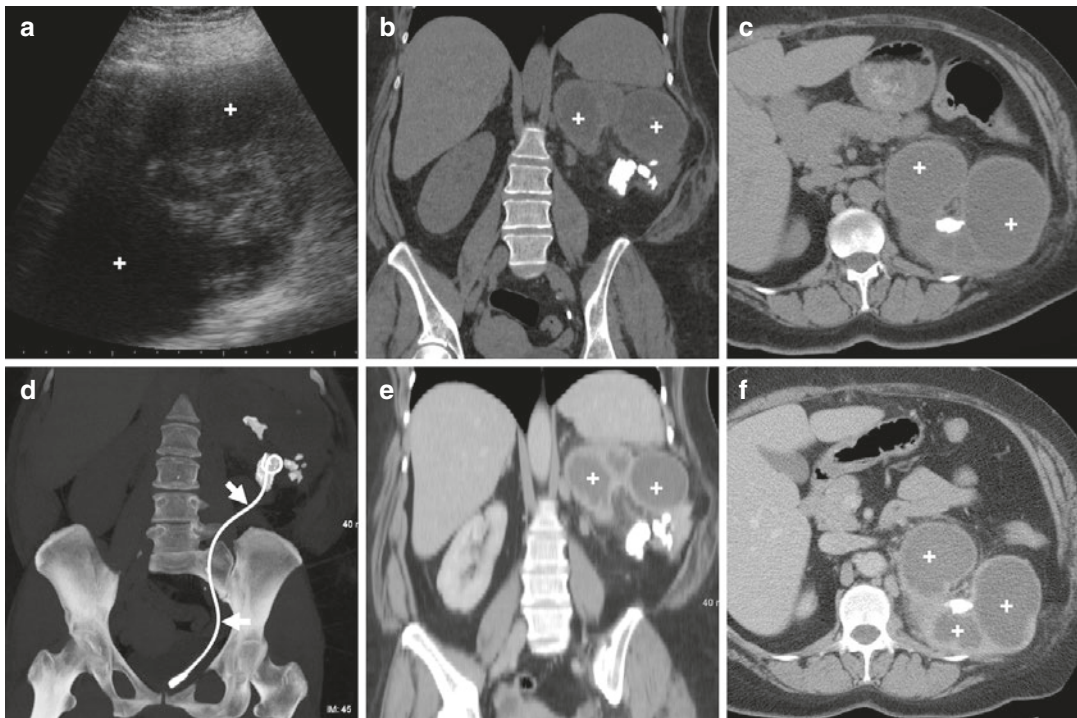


Fig. 10.8 A 48-year-old obese female with history of left-sided pyelolithotomy 15 years earlier was hospitalized with presumptive diagnosis of acute pyelonephritis. Ultrasound (a) showed extensive left renal replacement by large hypo-anechoic regions (plus) with poorly perceptible residual parenchyma. Unenhanced (b, c) CT images confirmed renal parenchymal thinning with sizeable, confluent water-attenuation cavities (plus) and 'staghorn' calcific lithiasis of the renal pelvis and upper and lower calyces. Ureteral stenting (thick arrows in (d)) was per-

formed to relieve pyonephrosis (as seen in maximum intensity projection (MIP) reconstruction). Six weeks later, after stent removal, contrast-enhanced CT (e, f) confirmed poorly enhancing renal parenchyma and uneven calyceal dilatation; the enlarged left kidney occupied and compressed the ipsilateral perirenal and pararenal spaces. After prolonged antibiotics, laparoscopic nephrectomy was performed. Histopathology diagnosed xanthogranulomatous pyelonephritis. (Adapted from Open Access ref.no [37])

the hydronephrotic pattern of the fluidlike cavities is crucial for a correct diagnosis. The highly specific fatty xanthomatous deposits with negative CT attenuation are detected in approximately 30% of cases. Contrast excretion into urine is rarely seen at diagnosis. Furthermore, CT readily detects extrarenal extension of XGPN into the perinephric space and other adjacent structures such as the posterior pararenal space and psoas muscles. Although less used in this setting, MRI may depict similar changes, with a lower sensitivity for nephrolithiasis. The pus-filled cavities show fluidlike very high T2-weighted signal intensity and variably hypointense T1 signal depending on the protein concentration; conversely the solid parts may be T1 isointense or hyperintense from adipose

component and iso- to slightly T2 hypointense [10, 11, 21, 32–38].

The combination of characteristic CT features, particularly:

- (a) Non-functioning kidney
- (b) Central lithiasis
- (c) Calyceal dilatation
- (d) Perinephric involvement

is strongly suggestive of XGPN, a diagnosis which is generally confirmed by histopathology on the nephrectomy specimen. The imaging diagnosis is challenging in atypical cases, such as in absence of calculi (10% of cases) and the rare (below 10% of cases) focal XGPN which appears

as a minimally enhancing renal mass and is commonly misinterpreted as bacterial abscess or tumour [10, 11, 21, 32–37].

10.4 Fistulising Renal Infections

Unrecognised acute or chronic pyelonephritis may further breach through the anterior or posterior renal fasciae and involve other retroperitoneal compartments, most often the posterior pararenal spaces, the iliopsoas and quadratus lumborum muscles (Fig. 10.9) and occasionally to the abdominal wall (Fig. 10.10) giving rise to more or less extensive abscess collections. Urinary tract fistulisation represents an abnormal communication between the renal parenchyma (nephro-) or the pelvis (pyelo-) and other structures: nowadays, the vast majority of urinary fistulas are iatrogenic in origin, secondary to surgical interventions or percutaneous procedures such as nephrostomy, nephrolithotomy or extracorporeal shock wave lithotripsy. Nowadays, cases of renal fistulas from penetrating trauma, tumours or infections are occasionally encountered [39, 40].

Multidetector CT represents the mainstay imaging modality to image fistulising complications, as it promptly provides a comprehensive diagnosis of retroperitoneal infectious involve-

ment even in acutely ill patients and in non-functioning kidneys and represents a consistent basis to choose between conservative, percutaneous or surgical treatment [41].

Muscular abscesses such as those involving the psoas present on cross-sectional imaging with variable enlargement of the muscle belly compared to the contralateral one. CT generally shows a hypoattenuating, sometimes multiloculated, lesion with peripheral ‘rim’ enhancement. Similarly, at MRI muscle abscesses appear as fluidlike cavities with low T1-weighted, high T2 signal intensity and strong ‘rim’ enhancement. Additional findings suggesting infection over haemorrhage or tumour include indistinct margins, obliteration of the surrounding fat planes and occasionally air-fluid levels; although uncommon, the presence of gas bubbles is considered specific [41–44].

Nowadays, psoas abscesses are most commonly secondary to direct infectious spread from adjacent organs such as the kidneys and urinary tract, the bowel, the lumbar spine or the aorta. When faced with a retroperitoneal abscess, the radiologist should suggest the likely cause between complicated urinary infection, gastrointestinal lesions, musculoskeletal and exceptionally aortic infections (Table 10.2). Generally encountered in association with HIV infection, intravenous drug abuse, immunosuppression or

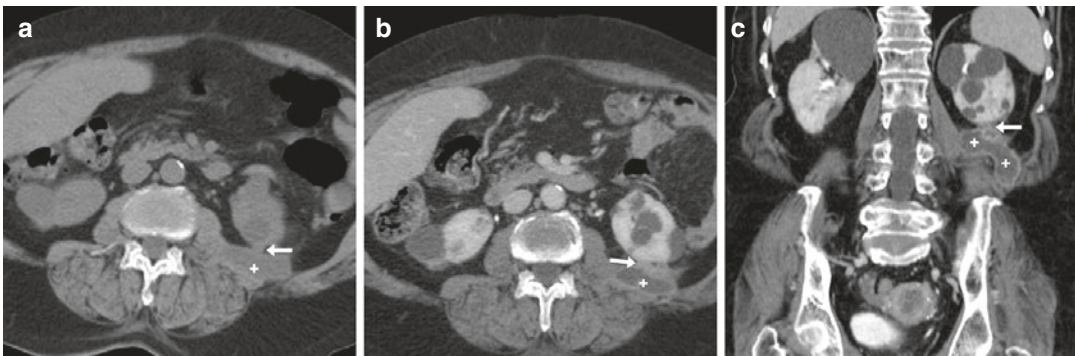


Fig. 10.9 A 78-year-old female with urinary infection and previously unknown multicystic chronic kidney disease underwent unenhanced (a) and post-contrast (b, c) multidetector CT. The posterior aspect of the left kidney was seen adherent and communicating (arrows) with an enlarged quadratus lumborum muscle (plus), character-

ised by fluidlike content and peripheral ‘rim’ enhancement consistent with muscle abscess from renal fistulisation. The patient did well with conservative treatment; the abscess was unchanged and anechoic at ultrasound follow-up (not shown)

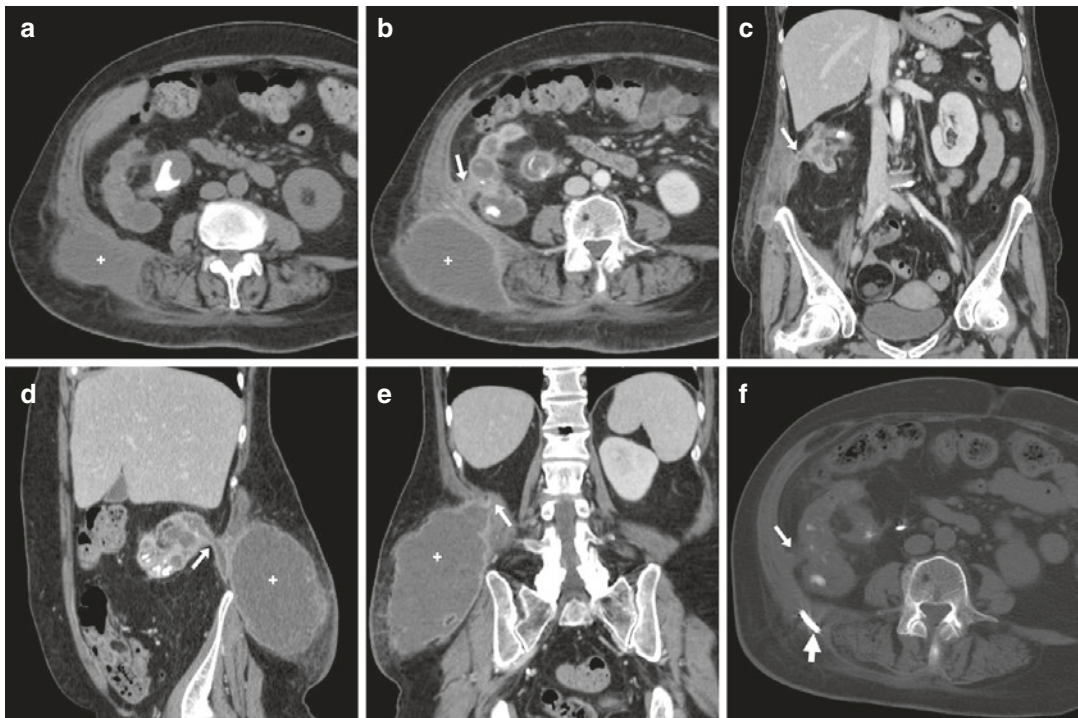


Fig. 10.10 A 64-year-old female presented to emergency department with low-grade fever and painful erythematous swelling in her right lumbar region, without any previous surgical or interventional procedures. Urgent unenhanced (a) and post-contrast (b–e) CT images showed right kidney with reduced, poorly functioning parenchyma, calcific pelvicalyceal stones. A fluid-containing track with enhancing walls (arrows) consistent with spontaneous fistulisation was seen crossing through

the perinephric, posterior pararenal spaces and abdominal wall muscles, to form a large abscess (plus) that displaced the superficial fascia. Percutaneous drainage (thick arrow in (f)) yielded 500 ml of pus from *P. mirabilis* infection. Follow-up unenhanced CT (f) confirmed disappearance of the abscess. Later on, laparoscopic nephroureterectomy was performed, and surgical pathology confirmed extensive renal infection breaching through the renal capsule

Table 10.2 Causes of psoas muscle abscesses

Source	Main underlying conditions
Urinary	Acute pyelonephritis
	Renal abscess
	Pyonephrosis
	Xanthogranulomatous pyelonephritis
Digestive tract	Fistulising Crohn's disease
	Colonic diverticulitis
	Complicated acute appendicitis
	Perforated colorectal cancer
Musculoskeletal	Pyogenic spondylodiskitis
	Spinal tuberculosis
	Infectious sacroiliitis
Vascular	Infected aortic aneurysms
	Prosthetic vascular infection
Haematogenous	Primary psoas abscess

DM, the rare primary iliopsoas abscesses originate from haematogenous spread and are diagnosed when no obvious local cause can be identified [44–46].

In current urological practice, spontaneous nephrocutaneous fistulas (NCFs) without history of surgery or other instrumentation are exceptionally encountered, invariably associated with long-standing nephrolithiasis and chronic UTI. A NCF involves the development of an abnormal communication between the kidney and the skin, classically crossing through the retroperitoneum and abdominal wall structures following the lowest resistance points such as Petit's triangle and the Grynfeld quadrilateral. Most reported cases are associated with 'staghorn' calculi and poorly functioning kidneys and attributed to XGPN,



Fig. 10.11 Four months after lithotripsy, a 45-year-old female with diabetes, HIV infection and ‘staghorn’ nephrolithiasis experienced a painful lumbar swelling. Careful inspection revealed a cutaneous ulcer on her left flank draining smelly greenish fluid. Compared to previous studies (not shown), contrast-enhanced multidetector CT (**a–c**) showed appearance of hydronephrosis with enhancing inflammatory urothelial thickening along the pelvis

and proximal and mid-ureter, a residual stone fragment (thin arrow in **(b)**) and ipsilateral adenopathies (arrowhead in **(a)**). Furthermore, a thin fluidlike track with enhancing wall (arrows in **(c)**) consistent with nephrocutaneous fistulisation was recognised, directed postero-inferiorly through the posterior pararenal space and abdominal wall to reach the skin orifice (Partially reproduced from Open Access Ref.no [39])

pyogenic infections such as renal abscesses or pyelocalyceal diverticula, tuberculosis, renal trauma or malignancies. The characteristic clinical manifestation is flank or lumbar tenderness and swelling with a cutaneous orifice draining urine or pus [47–52].

In the past, most patients were investigated with fluoroscopic retrograde pyelogram and or fistulography: the injected contrast medium directly opacified the abnormal tract and urinary collecting system, without providing any cross-sectional information on the involved renal and perirenal anatomical structures [40, 47, 51]. Conversely, CT comprehensively and noninvasively depicts the fistulous track even in poorly or non-functioning kidneys (Fig. 10.11). When contrast excretion is preserved, the NCF may be seen opacified on delayed excretory CT acquisitions obtained 20–120 min after intravenous injection. In the setting of urinary fistulisation, CT reliably provides:

- (a) Key information about size, parenchymal thickness and function of the involved kidney
- (b) Comprehensive characterisation and extent assessment of the underlying infectious or neoplastic disease

(c) A surgical road map for nephrectomy and fistula debridement

(d) Identification of abscesses amenable to drainage [40, 52]

Particularly in patients with non-functioning kidneys and complex lithiasis, nephrectomy plus fistulectomy is the standard surgical treatment which prevents sepsis, that should be planned after interventional treatment of pyonephrosis and abscesses with stenting or percutaneous drainage.

Conservative treatment with antibiotics is reserved for debilitated patients [47, 51].

References

1. Kumar S, Ramachandran R, Mete U et al (2014) Acute pyelonephritis in diabetes mellitus: single center experience. *Indian J Nephrol* 24:367–371
2. Garg V, Bose A, Jindal J et al (2015) Comparison of clinical presentation and risk factors in diabetic and non-diabetic females with urinary tract infection assessed as per the european association of urology classification. *J Clin Diagn Res* 9:PC12–PC14
3. Aboumarzouk OM, Hughes O, Narahari K et al (2014) Emphysematous pyelonephritis: time for a management plan with an evidence-based approach. *Arab J Urol* 12:106–115

4. Behera V, Vasantha Kumar RS, Mendonca S et al (2014) Emphysematous infections of the kidney and urinary tract: a single-center experience. *Saudi J Kidney Dis Transpl* 25:823–829
5. Dhabalia JV, Nelivigi GG, Kumar V et al (2010) Emphysematous pyelonephritis: tertiary care center experience in management and review of the literature. *Urol Int* 85:304–308
6. Sharma PK, Sharma R, Vijay MK et al (2013) Emphysematous pyelonephritis: our experience with conservative management in 14 cases. *Urol Ann* 5:157–162
7. Fatima R, Jha R, Muthukrishnan J et al (2013) Emphysematous pyelonephritis: a single center study. *Indian J Nephrol* 23:119–124
8. Lu YC, Hong JH, Chiang BJ et al (2016) Recommended initial antimicrobial therapy for emphysematous pyelonephritis: 51 cases and 14-year experience of a tertiary referral center. *Medicine (Baltimore)* 95:e3573
9. Tasleem AM, Murray P, Anjum F et al (2014) CT imaging is invaluable in diagnosing emphysematous pyelonephritis (EPN): a rare urological emergency. *BMJ Case Rep* 2014; bcr2014204040–bcr201420404
10. Demertzis J, Menias CO (2007) State of the art: imaging of renal infections. *Emerg Radiol* 14:13–22
11. Craig WD, Wagner BJ, Travis MD (2008) Pyelonephritis: radiologic-pathologic review. *Radiographics* 28:255–277. quiz 327–258
12. Stunell H, Buckley O, Feeney J et al (2007) Imaging of acute pyelonephritis in the adult. *Eur Radiol* 17:1820–1828
13. Portnoy O, Apter S, Koukoui O et al (2007) Gas in the kidney: CT findings. *Emerg Radiol* 14:83–87
14. Tsitouridis I, Michaelides M, Sidiropoulos D et al (2010) Renal emphysema in diabetic patients: CT evaluation. *Diagn Interv Radiol* 16:221–226
15. Huang JJ, Tseng CC (2000) Emphysematous pyelonephritis: clinicoradiological classification, management, prognosis, and pathogenesis. *Arch Intern Med* 160:797–805
16. Tonolini M, Vella A, Romanò AL, et al (2016) Emphysematous pyelonephritis in a solitary kidney. *EuroRAD* URL: <http://www.euro-rad.org/case.php?id=13869>
17. Alsharif M, Mohammedkhalil A, Alsaywid B et al (2015) Emphysematous pyelonephritis: is nephrectomy warranted? *Urol Ann* 7:494–498
18. Kangiam SM, Irom KS, Khumallambam IS et al (2015) Role of conservative management in emphysematous pyelonephritis - a retrospective study. *J Clin Diagn Res* 9:PC09–PC11
19. Lu YC, Chiang BJ, Pong YH et al (2014) Predictors of failure of conservative treatment among patients with emphysematous pyelonephritis. *BMC Infect Dis* 14:418
20. Browne RF, Zwirewich C, Torreggiani WC (2004) Imaging of urinary tract infection in the adult. *Eur Radiol* 14(Suppl 3):E168–E183
21. Das CJ, Ahmad Z, Sharma S et al (2014) Multimodality imaging of renal inflammatory lesions. *World J Radiol* 6:865–873
22. Ifergan J, Pommier R, Brion MC et al (2012) Imaging in upper urinary tract infections. *Diagn Interv Imaging* 93:509–519
23. Dunn DP, Kelsey NR, Lee KS et al (2015) Non-oncologic applications of diffusion-weighted imaging (DWI) in the genitourinary system. *Abdom Imaging* 40:1645–1654
24. Tonolini M, Ierardi AM, Carrafiello G (2015) Letter to the editor: spontaneous renal haemorrhage in end-stage renal disease. *Insights Imaging* 6:693–695
25. Diaz JR, Agriantoni DJ, Aguila J et al (2011) Spontaneous perirenal hemorrhage: what radiologists need to know. *Emerg Radiol* 18:329–334
26. Daskalopoulos G, Karyotis I, Heretis I et al (2004) Spontaneous perirenal hemorrhage: a 10-year experience at our institution. *Int Urol Nephrol* 36:15–19
27. Zhang JQ, Fielding JR, Zou KH (2002) Etiology of spontaneous perirenal hemorrhage: a meta-analysis. *J Urol* 167:1593–1596
28. Tittton RL, Gervais DA, Hahn PF et al (2003) Urine leaks and urinomas: diagnosis and imaging-guided intervention. *Radiographics* 23:1133–1147
29. Gayer G, Zissin R, Apter S et al (2002) Urinomas caused by ureteral injuries: CT appearance. *Abdom Imaging* 27:88–92
30. Heller MT, Haarer KA, Thomas E et al (2012) Acute conditions affecting the perinephric space: imaging anatomy, pathways of disease spread, and differential diagnosis. *Emerg Radiol* 19:245–254
31. Hartman DS, Choyke PL, Hartman MS (2004) From the RSNA refresher courses: a practical approach to the cystic renal mass. *Radiographics* 24(Suppl 1):S101–S115
32. Loffroy R, Guiu B, Watfa J et al (2007) Xanthogranulomatous pyelonephritis in adults: clinical and radiological findings in diffuse and focal forms. *Clin Radiol* 62:884–890
33. Zorzos I, Moutzouris V, Korakianitis G et al (2003) Analysis of 39 cases of xanthogranulomatous pyelonephritis with emphasis on CT findings. *Scand J Urol Nephrol* 37:342–347
34. Rajesh A, Jakanani G, Mayer N et al (2011) Computed tomography findings in xanthogranulomatous pyelonephritis. *J Clin Imaging Sci* 1:45
35. Kim JC (2001) US and CT findings of xanthogranulomatous pyelonephritis. *Clin Imaging* 25:118–121
36. Yu M, Robinson K, Siegel C et al (2016) Complicated genitourinary tract infections and mimics. *Curr Probl Diagn Radiol* 46(1):74–83. <https://doi.org/10.1067/j.cpradiol.2016.1002.1004>
37. Tonolini M, Bonzini M (2016) Xanthogranulomatous pyelonephritis: when CT findings suggest the diagnosis. *EuroRAD* URL: <http://www.euro-rad.org/case.php?id=14129>
38. Nikken JJ, Krestin GP (2007) MRI of the kidney-state of the art. *Eur Radiol* 17:2780–2793
39. Tonolini M, Villa F, Ippolito S et al (2014) Cross-sectional imaging of iatrogenic complications after

- extracorporeal and endourological treatment of urolithiasis. *Insights Imaging* 5:677–689
40. Yu NC, Raman SS, Patel M et al (2004) Fistulas of the genitourinary tract: a radiologic review. *Radiographics* 24:1331–1352
 41. Tonolini M, Campari A, Bianco R (2012) Common and unusual diseases involving the iliopsoas muscle compartment: spectrum of cross-sectional imaging findings. *Abdom Imaging* 37:118–139
 42. Zissin R, Gayer G, Kots E et al (2001) Iliopsoas abscess: a report of 24 patients diagnosed by CT. *Abdom Imaging* 26:533–539
 43. Muttarak M, Peh WC (2000) CT of unusual iliopsoas compartment lesions. *Radiographics* 20(Suppl 1):S53–S66
 44. Cronin CG, Lohan DG, Meehan CP et al (2008) Anatomy, pathology, imaging and intervention of the iliopsoas muscle revisited. *Emerg Radiol* 15:295–310
 45. van den Berge M, de Marie S, Kuipers T et al (2005) Psoas abscess: report of a series and review of the literature. *Neth J Med* 63:413–416
 46. Mallick IH, Thoufeeq MH, Rajendran TP (2004) Iliopsoas abscesses. *Postgrad Med J* 80:459–462
 47. Antunes AA, Calado AA, Falcao E (2004) Spontaneous nephrocutaneous fistula. *Int Braz J Urol* 30:316–318
 48. Ansari MS, Singh I, Dogra PN (2004) Spontaneous nephrocutaneous fistula--2 unusual case reports with review of literature. *Int Urol Nephrol* 36:239–243
 49. Singer AJ (2002) Spontaneous nephrocutaneous fistula. *Urology* 60:1109–1110
 50. Qureshi MA (2007) Spontaneous nephrocutaneous fistula in tuberculous pyelonephritis. *J Coll Physicians Surg Pak* 17:367–368
 51. Charles JC (1990) Nephrocutaneous fistula. *J Natl Med Assoc* 82:589–590
 52. Cooper SG, Richman AH, Tager MG (1989) Nephrocutaneous fistula diagnosed by computed tomography. *Urol Radiol* 11:33–36
 53. Tonolini M (2011) Spontaneous perinephric urinoma complicating obstructive uropathy {Online}. EuroRAD URL: <http://www.eurorad.org/case.php?id=9710>